Evaluation of Respiratory Triggering Algorithms

W. M. Skeffington[1], R. F. Busse[1], J. W. Johnson[1], R. H. Herfkens[2], J. H. Brittain[1]

[1]Applied Science Lab - West, GE Medical Systems, Menlo Park, CA, United States, [2]Dept. of Radiology, Stanford University, Stanford, CA, United States

Introduction

In many abdominal applications, data for any given image is collected over a number of respiratory cycles. If the anatomy does not return to a consistent location from cycle to cycle, image artifact results [1]. Respiratory triggering [2] is a method to use physiologic monitoring (from, for instance, a bellows device or navigator echo [3]) to synchronize the acquisition to the respiratory cycle. Because breathing is not perfectly periodic [4], algorithms which analyze the respiratory data need to be sophisticated enough to recognize and react to changes in respiratory rate and local minima and maxima in the waveforms. We investigated two algorithms that generate data acquisition triggers from respiratory data.

Methods

Both algorithms investigated were designed to trigger data acquisition during expiration. Algorithm I identified inspiration peaks and then waited a set period (user-defined percentage of the estimated respiratory period) before sending a trigger signal. Algorithm II analyzed the respiratory position signal (p) and the first and second derivative of the signal (p' and p'') to identify transitions in a finite state machine. There were four defined states identified in sequence: Identify Peak Inspiration, Identify Begin of Acquisition Window (trigger-point), Identify Peak Expiration, and Identify End of Acquisition Window. Transitions out of states Peak Inspiration and Peak Expiration were based on respiration p, p', and p''; while transitions from states Begin of Acquisition Window and End of Acquisition Window were established on respiration p' and a user-defined respiration threshold p (T). Process maps for the two algorithms are shown in Figure 1-A and Figure 1-B. Figure 2 illustrates a typical respiration waveform and the operation of Algorithm II's state machine.

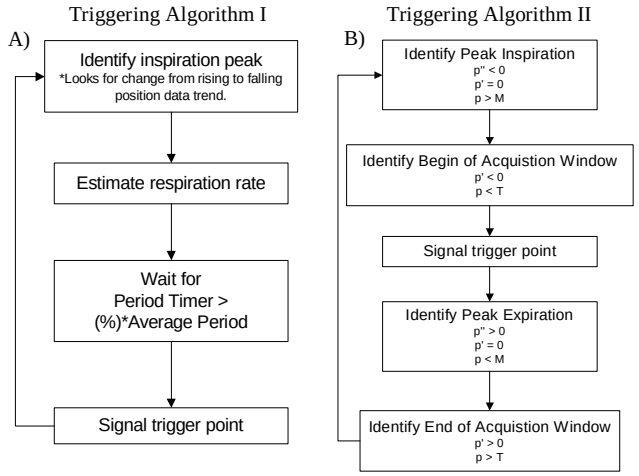

Figure 1 – Algorithm Process Maps

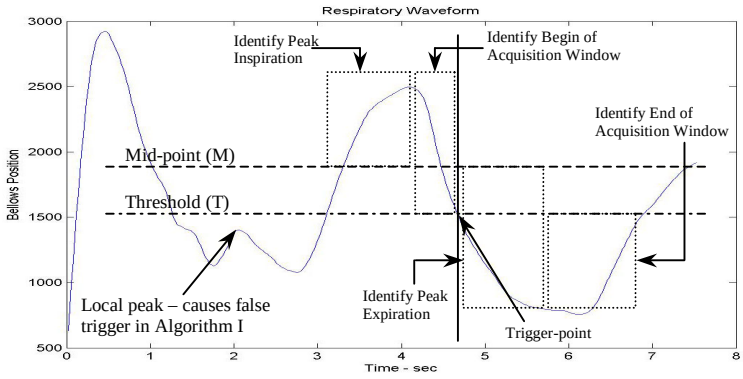

Figure 2 – Respiratory Waveform – Algorithm II State Machine Map

$$\sigma_t^2 = \frac{1}{R}\sum_{r=1}^{R}\left|x_{r,t} - \mu_t\right|^2 \quad \text{(Eq. 1)} \qquad \sigma_{aw} = \frac{1}{T}\sum_{t=1}^{T}\sigma_t \quad \text{(Eq. 2)}$$

r ≡ respiratory cycle index
R ≡ total number of respiratory cycles
μ_t ≡ chest position average at time point t
T ≡ data acquisition window length

Respiratory waveforms generated by a bellows device on a GE 1.5T *Signa EXCITE* scanner (GE Medical Systems, Milwaukee, WI) were collected from five volunteers and five patients. These data were input to both algorithms to determine where the trigger points fell and how the respiratory signal varied for the acquisition period following the trigger. Analysis and comparison of the two algorithms was conducted in a MATLAB simulation environment. Although in the cases presented the data was collected from a bellows type technology, both algorithms could be used in conjunction with any method of measuring respiratory motion as a function of time including bellows, navigators, or respiratory pillows.

For this analysis, we assumed that variation in chest position (as measured by bellows) was well correlated to physiological position. We also assumed that data for a given slice were acquired instantaneously at some time t after the trigger and of chief importance to image quality was the consistency of position from repetition to repetition (cycle to cycle) at that time t. A metric σ_t (see Eq. 1) was derived to measure positional consistency at each time t. The average consistency over all t in the acquisition window, σ_{aw} (see Eq. 2), was used as a metric for overall data consistency.

Results

Figure 2 demonstrates an example of Algorithm I's vulnerability to local minima and maxima. Such events cause trigger points at times of inspiration, leading to imaging when the anatomy is not in a consistent position. Algorithm I is also inherently susceptible to failure due to changes in respiration frequency, whereas Algorithm II functions independently of respiration rate, and is therefore not prone to such failures.

Figure 3-A shows a comparison of σ_t between Algorithm I and Algorithm II in a single 60-second (15 respiratory cycles) data set. For this patient, Algorithm II identified a data acquisition window with lower variation in chest position for all t in the acquisition window. Figure 3-B shows a comparative analysis of σ_{aw} over ten data sets. Algorithm II produced superior results for 90% of the analyzed data sets and the average improvement in σ_{aw} was 44%.

Continuing work will include a blinded study in a clinical setting to better understand algorithm effects on image quality. We will also investigate Algorithm II's ability to directly measure and then estimate optimal data acquisition window length, given a user-defined threshold (T); this could lead to further improvements in image quality and scan time efficiency.

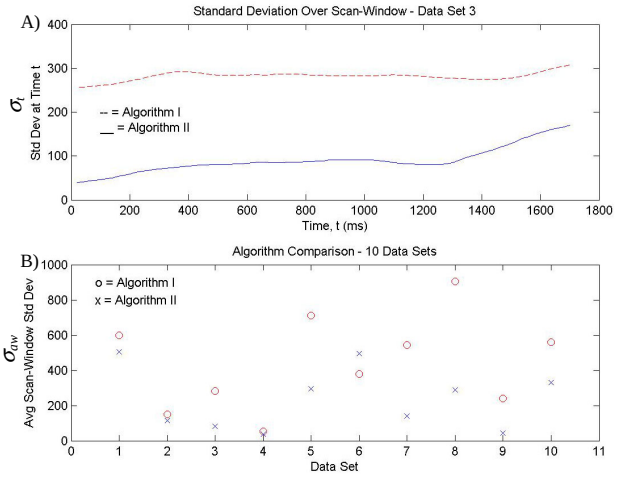

Figure 3 – Quantitative Algorithm Comparison

References

(1) Wood ML, Henkelman RM. Med Phys. 1985; 12:143-151.
(2) Lewis CE, et al. Radiology. 1986; 60(3):803-810.
(3) Ehman RL, Felmlee JP. Radiology. 1989; 173:255-263.
(4) Lauzon ML, et al. J Magn Reson Imaging. 1994; 4(6):853-67.